

## Durham Research Online

---

### Deposited in DRO:

03 June 2021

### Version of attached file:

Accepted Version

### Peer-review status of attached file:

Peer-reviewed

### Citation for published item:

Evans, John S. O. and Radosavljevic Evans, Ivana (2021) 'Structure Analysis from Powder Diffraction Data: Rietveld Refinement in Excel.', *Journal of Chemical Education*, 98 (2). pp. 495-505.

### Further information on publisher's website:

<https://doi.org/10.1021/acs.jchemed.0c01016>

### Publisher's copyright statement:

This document is the Accepted Manuscript version of a Published Work that appeared in final form in *Journal of Chemical Education*, copyright © American Chemical Society after peer review and technical editing by the publisher. To access the final edited and published work see <https://doi.org/10.1021/acs.jchemed.0c01016>

### Additional information:

---

### Use policy

The full-text may be used and/or reproduced, and given to third parties in any format or medium, without prior permission or charge, for personal research or study, educational, or not-for-profit purposes provided that:

- a full bibliographic reference is made to the original source
- a [link](#) is made to the metadata record in DRO
- the full-text is not changed in any way

The full-text must not be sold in any format or medium without the formal permission of the copyright holders.

Please consult the [full DRO policy](#) for further details.

---

# Structure Analysis from Powder Diffraction Data: Rietveld Refinement in Excel

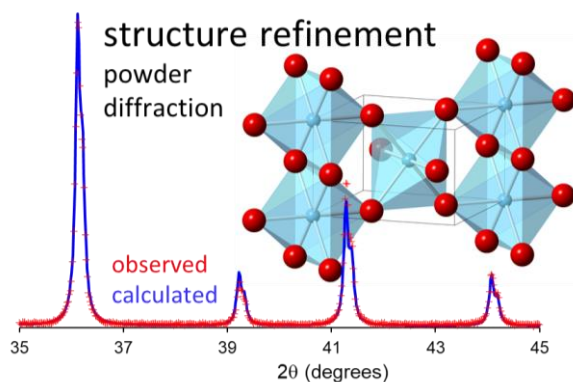
John S. O. Evans\* and Ivana Radosavljevic Evans

Department of Chemistry, Durham University, Science Site, South Road, Durham DH1 3LE, U.K.

## ABSTRACT

Powder diffraction is one of the most widely used analytical techniques for characterizing solid state materials. It can be used for phase or polymorph identification, quantitative analysis, cell parameter determination or even full crystal structure analysis using the powerful Rietveld refinement method. As with much of modern crystallography, the software used for Rietveld refinement is frequently treated as a "black box" that produces often-poorly-understood outputs. This paper shows how it is possible for students to perform a full Rietveld refinement against experimental powder diffraction data from scratch using a simple spreadsheet like Excel. It starts by reviewing the basic ideas of least-squares fitting a straight line, develops these into fitting simple functions to peaks in simulated experimental data, then combines these ideas with crystallographic equations to enable Rietveld refinement of the structure of an inorganic material (rutile,  $\text{TiO}_2$ ). At each stage students can self-learn different fundamental aspects and pitfalls of data analysis that are widely re-applicable. The ideas can be taught as an online learning exercise, or could be incorporated in a laboratory class where students collect and analyze their own experimental data.

## GRAPHICAL ABSTRACT



---

## KEYWORDS

Upper-Division Undergraduate, Graduate Education/Research, Laboratory Instruction, Computer-Based Learning, Materials Science, Solid State Chemistry, Inorganic Chemistry, Physical Chemistry, X-ray Crystallography

### 1. INTRODUCTION

X-ray and neutron diffraction are amongst the most powerful analytical techniques for probing chemical structure in the solid state, and are widely used in academic, industrial and environmental research ranging from the fundamental to the applied. The breadth and importance of the techniques is exemplified by the Cambridge Structural Database, which contains over 1,000,000 organic/organometallic entries that have been crystallographically characterized<sup>1</sup>; the ICSD which contains over 200,000 inorganic crystal structure;<sup>2</sup> and the International Centre for Diffraction Data's Powder Diffraction File PDF-4,<sup>3</sup> which contains >425,000 inorganic entries. As such, the fundamentals of crystallography are taught on many undergraduate chemistry, physics, engineering, materials, pharmaceutical science and life science courses. One of the challenges in enthusing students about crystallographic methods is that the data analysis required to go from experimental data to a final structural model relies on sophisticated and specialized software that has a steep learning curve. The result is that such software is often treated by users as a black box. It also leads to significant gaps developing between the theory students see in lectures and text books, and the way they experience crystallography in a practical setting. Several publications have previously raised the educational consequences, and there have been a number of earlier papers on how to build crystallographic education into school, undergraduate and postgraduate curricula.<sup>4-15</sup> Several previous publications have described ways in which powder diffraction experiments can be introduced into undergraduate practical classes to highlight the importance of the technique itself,<sup>6, 16-18</sup> or its use as a characterization method as part of a wider laboratory practical.<sup>19-23</sup> We are, however, unaware of other work that teaches structure analysis from powder diffraction data in the way described here.

The paper is based on a training exercise we have run on graduate-level schools over the last ten years, but is equally appropriate for advanced undergraduate students. It guides students from the very general ideas of data analysis to the point where they can perform a full Rietveld structural analysis on a simple material using nothing more than Microsoft Excel's built-in "Solver" function. By

---

50 working from experimental data right through to a three dimensional structure, students learn many of the key aspects of crystallographic analysis, as well as least-squares fitting skills that are widely re-applicable in other areas. By performing all steps in the data analysis from the bottom-up they learn through experience how crystallographic refinements work, and how they can fail. As such, we hope that the paper will help address many of the educational issues outlined in the previous paragraph.

55 The paper is organized into eight main sections (see Figure 1) allowing instructors to tailor training depending on the students' background and the time available. Section 2 gives a brief overview of diffraction and includes the important equations that are used in later data analysis. Section 3 describes the ideas behind whole-powder-diffraction-pattern fitting methods such as Rietveld and Pawley/Le Bail refinement.<sup>24-26</sup> These sections contain the background information students need to  
60 understand the work, or that non-specialist teaching assistants (TAs) will need to support student learning. Section 4 gives a very basic introduction to least-squares fitting using Excel's Solver function, then explores fitting either linear or non-linear functions to experimental data. Section 5 takes the ideas of data fitting and develops them into fitting experimental peaks using the commonly-used Gaussian or Lorentzian functions. Section 6 then explores how to fit multiple peaks in a dataset  
65 at either freely-refined positions or, as in powder diffraction analysis, at positions determined by the size and shape of a unit cell. We then introduce the constraint that the peak intensities are determined by the types of atoms and their positions in the unit cell, allowing a structural model to be least-squares fitted to an experimental data set—Rietveld refinement. Since Rietveld refinement is the ultimate goal of the paper it is treated in most detail, and students could choose to skip the earlier  
70 parts of Section 6. Section 7 allows students to perform a Rietveld refinement on real experimental data, either provided in the accompanying Excel spreadsheet, or that they collect themselves. Finally, Section 8 summarizes our learning from using these exercises in a classroom setting and our assessment of their effectiveness.

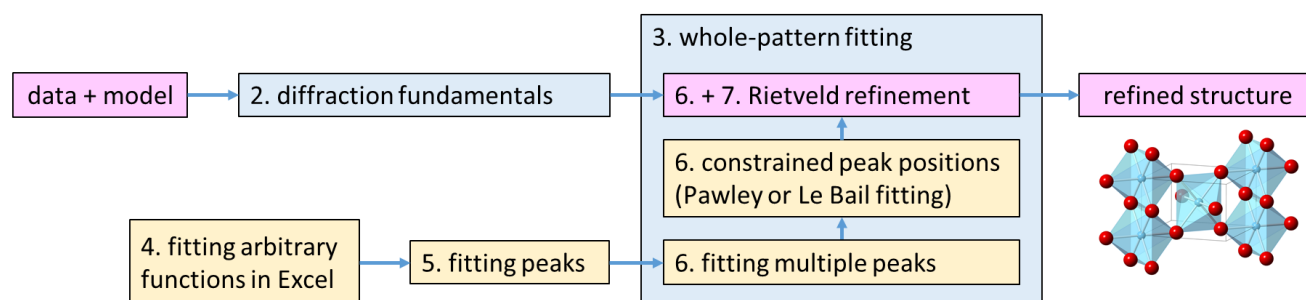


Figure 1. A schematic of how the different Sections of the paper interact: the background theory in Sections 2 and 3 (shaded blue) allow students to build-up the complexity of data analysis through Sections 4, 5 and 6 (yellow boxes); they can then achieve the goal of going directly from experimental data and a model structure to a final Rietveld-refined structure (pink boxes).

We have tried to include sufficient information that the sections of the paper targeted at students can be read as a stand-alone manuscript, and have kept the paper's mathematical and crystallographic content at the minimum level we believe is needed for students to understand the process. We are aware that we have omitted many important details for brevity, so provide references to more detailed texts where appropriate.

We have provided an Excel spreadsheet as Supplementary Information which contains all the data, instructions and equations needed to work through each example, and which contains "pop-up help boxes" for students. We have also provided instructor/TA notes in the Supplementary Information which outline the tasks students could follow, sets "challenge questions" and suggests discussion points at different stages. Corresponding step-by-step tutorials are available online.<sup>27</sup> We also provide example datafiles so students could repeat this analysis in widely-used specialist software packages for Rietveld refinement.

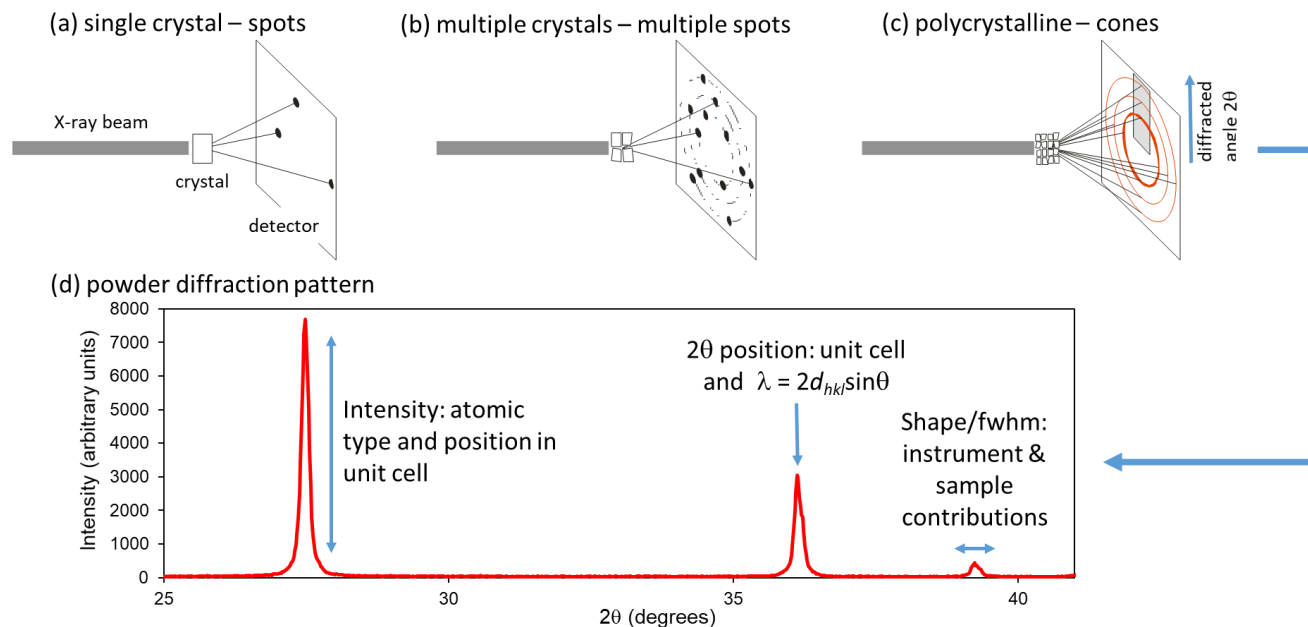


Figure 2. A single crystal gives rise to diffracted beams in discrete directions which appear as "spots" on a 2D detector. With multiple crystals, spots will be seen from each crystal. In a powdered or polycrystalline sample this leads to cones of diffracted intensity which are intersected as circles on a 2D detector, each circle corresponds to an individual or overlapped set of  $hkl$  reflections. A one-dimensional scan in  $2\theta$  across these rings (or integration around them) leads to (d) a powder diffraction pattern as a plot of diffracted intensity as a function of angle  $2\theta$ .

## 2. DIFFRACTION FUNDAMENTALS

When electromagnetic radiation with a wavelength comparable to interatomic separations is incident on a crystalline sample, each atom acts as a source of scattered radiation and the constructive/destructive interference between the scattered waves leads to diffraction. If we picture a crystal as containing planes described by Miller indices ( $hkl$ ), Bragg's law gives the angle of constructively scattered intensity via:

$$\lambda = 2d_{hkl}\sin\theta \quad (1)$$

where  $\lambda$  is the wavelength,  $d_{hkl}$  the interplanar spacing and  $2\theta$  the direction relative to the incident beam. For any crystal system,  $d_{hkl}$  can be related to the unit-cell parameters  $a$ ,  $b$ ,  $c$ ,  $\alpha$ ,  $\beta$ ,  $\gamma$  by trigonometry. For a tetragonal unit cell ( $a = b \neq c$ ;  $\alpha = \beta = \gamma = 90^\circ$ ), the general expression simplifies to:

$$\frac{1}{d_{hkl}^2} = \frac{h^2 + k^2}{a^2} + \frac{l^2}{c^2} \quad (2)$$

Equations (1) and (2) tell us that the possible angles of diffracted intensity ( $2\theta_{hkl}$ ) in any diffraction pattern depend solely on the size and shape of the unit cell. For a single crystal we get beams of diffracted intensity in specific directions when Bragg's law is satisfied. For a polycrystalline material,

the random orientation of crystallites (Figure 2) means that these beams become averaged into concentric cones. In a traditional powder diffraction experiment, a detector is scanned across these cones to produce a plot of diffracted intensity versus angle  $2\theta$ —a powder diffraction pattern. For data analysis patterns are normally treated as a series of  $y_{obs,i}$  intensity values at  $N$  discrete  $2\theta$  steps.

The intensity  $I_{hkl}$  of each  $hkl$  reflection is determined by the identity and positions of the atoms inside the unit cell via the structure factor,  $F_{hkl}$ :

$$F_{hkl} = \sum_j t_j f_j \exp[2\pi i(hx_j + ky_j + lz_j)] \quad (3)$$

$$I_{hkl} \propto |F_{hkl}|^2 \quad (4)$$

Here  $x_j, y_j, z_j$  are fractional atomic coordinates of atom  $j$ , and  $f_j$  describes the scattering factor of atom  $j$  as a function of  $\sin\theta/\lambda$ . The  $t_j$  term accounts for the fact that atoms vibrate around their average positions in real samples, which decreases  $I_{hkl}$  intensities. In this paper we will use an isotropic correction  $t_j = \exp(-B \sin^2\theta/\lambda^2)$ , where the atomic displacement parameter  $B$  (the "temperature factor" or "Debye-Waller" factor) is expressed as  $B = 8\pi^2 u^2$ , and  $u$  is the root mean squared atomic displacement in Å. It's worth noting that this parameter is typically poorly determined from laboratory powder X-ray data—over a short  $2\theta$  range  $B$  correlates highly with the overall scale factor, and can be strongly affected by factors such as the sample absorption and any surface roughness in a reflection geometry experiment.

For a powder diffraction experiment, several factors usually appear in the  $I_{hkl} \propto |F_{hkl}|^2$  proportionality constant: an overall scale factor, factors describing the diffractometer geometry in the so-called LP or Lorentz-polarization factor, and the reflection multiplicity  $m$ .  $m$  counts the number of symmetry equivalent reflections for each  $hkl$ . For example, in a tetragonal system, the (110) reflection has multiplicity 4 [(110), (-1-10), (-110), (1-10)]. All of these terms are described in full detail in most crystallography texts.<sup>24, 28-30</sup>

In this paper we ultimately explore the example of rutile  $\text{TiO}_2$ , using diffraction data recorded on a powder diffractometer with Cu  $K_\alpha$  radiation produced by a graphite monochromator set at an angle ( $2\theta_{\text{mono}}$ ) of  $26.6^\circ$ . Rutile is tetragonal, space group  $P4_2/mnm$ , has  $a \approx 4.6$  Å  $c \approx 2.96$  Å and contains Ti

on Wyckoff site  $2a$  (0, 0, 0) [symmetry generates a second atom at  $(\frac{1}{2}, \frac{1}{2}, \frac{1}{2})$ ] and an oxygen on  $4f$  ( $x, x, 0$ ) with  $x \approx 0.3$  [symmetry generates  $(-x, -x, 0)$ ,  $(-x + \frac{1}{2}, x + \frac{1}{2}, \frac{1}{2})$ ,  $(x + \frac{1}{2}, -x + \frac{1}{2}, \frac{1}{2})$ ;  $x = 0.30631$  was used for simulated datasets]. For this example, the intensity of each  $hkl$  reflection<sup>31</sup> can be calculated using the following equations:

$$I_{hkl} = scale \times LP \times m \times F_{hkl}^2 \quad (5)$$

$$F_{hkl} = t_{Ti} f_{Ti} A_{Ti} + t_O f_O A_O \quad (6)$$

$$A_{Ti} = 2 \cos^2 2\pi \left( \frac{h+k+l}{4} \right) \quad (7)$$

$$A_O = 2 \cos 2\pi l z \left[ \cos 2\pi \left( hx - \frac{h+k+l}{4} \right) \cos 2\pi \left( ky + \frac{h+k+l}{4} \right) \cos 2\pi \left( kx - \frac{h+k+l}{4} \right) \cos 2\pi \left( hy + \frac{h+k+l}{4} \right) \right] \quad (8)$$

$$t_j = \exp \left( \frac{-B_j \sin^2 \theta}{\lambda^2} \right) \quad (9)$$

$$LP = \frac{1 + \cos^2 2\theta_{\text{mono}} \cos^2 2\theta}{\sin^2 \theta \cos \theta}; 2\theta_{\text{mono}} = 26.6^\circ \quad (10)$$

Equations 6–8 are a simplification of the more general Equation 3 for this specific structure, and allow us to use just the symmetry-unique atoms in calculations.

In any real diffraction experiment, each  $hkl$  reflection is observed over a small range of  $2\theta$  values giving a peak of finite width. The shape of the peak is caused by a combination (strictly a convolution) of effects from the radiation source, the diffractometer components and the sample.<sup>24</sup> Whilst the details of peak shape can be of enormous scientific importance, we will just take an empirical approach and state that peaks can often be described analytically by either Gaussian or Lorentzian functions, or by some combination of the two (e.g., a Voigt or pseudo-Voigt function). For this paper we adopt the unit area peak shape definitions given by Young:<sup>26</sup>

$$G = \frac{C_0^{1/2}}{fwhm \cdot \pi^{1/2}} \exp \left( \frac{-C_0 (2\theta - 2\theta_{hkl})^2}{fwhm^2} \right) \quad (11)$$

$$L = \frac{C_1^{1/2}}{fwhm \cdot \pi} 1 / \left[ 1 + C_1 \frac{(2\theta - 2\theta_{hkl})^2}{fwhm^2} \right] \quad (12)$$

$$pV = \eta L + (1 - \eta)G \quad (13)$$



where  $C_0 = 4 \ln 2$ ,  $C_1 = 4$ ,  $2\theta$  the diffraction angle in question,  $2\theta_{hkl}$  the peak position and  $\eta$  a mixing parameter. The peak full width at half maximum (*fwhm*) usually varies smoothly with  $2\theta$ .

### 3. WHOLE-POWDER-PATTERN FITTING AND RIETVELD REFINEMENT

Whilst single crystal diffraction is considered the gold standard for determination of crystal structures, powder diffraction has many of its own distinct advantages: for many compounds it can be difficult or impossible to grow diffraction-quality single crystals; samples can be readily studied under real working conditions (e.g. *operando* catalysis / batteries); samples can be studied through phase transitions where single crystals would be destroyed; and multi-phase samples can be studied allowing qualitative or quantitative phase analysis.<sup>32</sup> For these reasons, powder diffraction<sup>33-34</sup> has often provided the crucial break-through structural insights in diverse areas such as high temperature superconductors, batteries and energy materials, ferroelectric materials, zeolite chemistry, negative thermal expansion, pharmaceutical polymorphism and many others.

The most commonly cited disadvantage of powder diffraction is that the three dimensional diffraction data of a single crystal is compressed onto the single dimension of the diffraction angle  $2\theta$ , meaning that different  $hkl$  reflections often overlap in  $2\theta$ . This overlap means that, in contrast to single crystal methods, it can be difficult or impossible to experimentally determine the accurate intensities of individual reflections needed for structural analysis. The solution to this problem is to adopt a whole-pattern fitting approach in which a structural model, a description of the peak shapes, and parameters to describe the background are used to calculate a powder pattern. The calculated intensity,  $y_{calc,i}$  at each step in  $2\theta$  is then compared to the observed intensity  $y_{obs,i}$  and the difference between the two minimized by changing certain parameters of the model. This is most commonly done by a least-squares refinement in which the quantity minimized is:

$$\sum_{i=1}^N w_i (y_{obs,i} - y_{calc,i})^2 \quad (14)$$

This is an iterative multi-step process in which the model (hopefully) improves in each cycle of refinement and is used to initiate a subsequent minimization cycle. The process is normally followed by monitoring the weighted profile R factor,  $R_{wp}$ , which should tend to a low value:

$$R_{wp} = \sqrt{\frac{\sum_{i=1}^N w_i (y_{obs,i} - y_{calc,i})^2}{\sum_{i=1}^N w_i y_{obs,i}^2}} \quad (15)$$

185 or a quantity such as goodness of fit (GoF) or  $\chi$ , which relates  $R_{wp}$  to the statistically expected value  $R_{exp}$ :

$$GoF = \chi = \frac{R_{wp}}{R_{exp}} = \sqrt{\frac{\sum_{i=1}^N w_i (y_{obs,i} - y_{calc,i})^2}{N - P}} \quad (16)$$

where  $N$  is the number of data points and  $P$  the number of parameters.  $\chi$  should tend to 1 for a good refinement. Least-squares uses a  $1/\sigma(y_{obs,i})^2$  weighting, where  $\sigma(y_{obs,i})$  is the experimental uncertainty  
 190 in  $y_{obs,i}$ . A diffraction pattern recorded on a conventional powder diffractometer with a point detector will typically follow Poisson statistics such that  $\sigma(y_{obs,i}) = \sqrt{y_{obs,i}}$ ; the resulting  $1/y_{obs,i}$  weighting is assumed for all the powder diffraction examples in the paper.

Common parameters refined when fitting the data include structural parameters (the sample unit-cell parameters, fractional atomic coordinates, atomic site occupancies and atomic displacement  
 195 parameters), parameters describing the instrument calibration (e.g. any  $2\theta$  zero-point offset), parameters describing any  $2\theta$ -dependent intensity correction (e.g. due to absorption), parameters describing the peak shape, and parameters describing the background between the Bragg peaks. The method was first coded by Hugo Rietveld and is usually referred to as Rietveld refinement.<sup>35-38</sup>

There are a few other important whole-pattern fitting methods used in powder diffraction analysis.  
 200 One is to simply freely refine the  $2\theta$  values and intensities of peaks to describe each reflection without a structural model. This can be a good way to obtain peak  $2\theta$  positions, which can be used to determine unit-cell parameters in a process called auto-indexing. Problems can arise as a result of the large number of parameters when there is significant peak overlap. Another is to adjust the intensity of each reflection but at  $2\theta$  values constrained by a unit cell and  $hkl$  indices. This approach can  
 205 substantially reduce the number of parameters relative to free peak fitting, and lets you decide the best fit possible to an experimental data set for a given unit cell. Methods to achieve this are usually called Pawley or Le Bail fitting, and the differences in the underlying algorithms of the two methods are explained in the references.<sup>24, 39-41</sup>

---

It is also worth noting that we need a starting structural model for Rietveld refinement in order to produce a reasonable initial calculated powder diffraction pattern. Structure solution is outside the main scope of this paper, but we could use the peak intensities from whole-profile fitting and single-crystal like methods (e.g. direct methods, charge flipping) to come up with a structural model.<sup>42</sup> Alternatively there are a variety of methods now available for rapidly testing computer-generated guessed structures against experimental data to find a plausible starting model;<sup>42</sup> students can explore this in the final part of Section 6. However, the most common approach is to use an approximate structural model derived from a related compound.

#### 4. AN INTRODUCTION TO LEAST-SQUARES FITTING

We normally have students start with a simple artificial example of model fitting, but one which illustrates the general approach and teaches some important pitfalls. Let's take the first two columns in Table 1 from a simple "experiment" and plot the data (Figure 3a, blue points). The values could represent the number of flowers on a rose bush on a given day. If we wanted a simple model to predict the number of flowers on day 5, we could fit a linear expression  $y = mx + c$  to obtain the gradient ( $m = 5.3$ ) and intercept ( $c = -4.5$ ) allowing us to predict the number of flowers on day 5 as 22. In Excel the normal approach would be to "right click on plot, add trendline". What Excel is actually doing here is minimizing  $\sum_i (y_{obs,i} - y_{calc,i})^2$  for all data points by adjusting or refining the values of  $m$  and  $c$  in a process called least-squares refinement. In other words, it minimizes Equation 14 under the assumption of equal weights for each experimental observation.

As illustrated in the accompanying Excel spreadsheet, students can do the same thing more explicitly in Excel using its built-in Solver routine. In the spreadsheet *solver\_linear\_fit* they can define values for  $m$  and  $c$  in individual cells. For each value of  $x$  they can create columns containing  $y_{obs}$ ,  $y_{calc}$  ( $=mx + c$ ),  $(y_{obs} - y_{calc})$  and  $(y_{obs} - y_{calc})^2$ . They can create a cell containing the sum of the  $(y_{obs} - y_{calc})^2$  column [or use the Excel SUMSQ function on  $(y_{obs} - y_{calc})$ ], and use Solver to minimize this cell by varying the cells containing  $m$  and  $c$ . This gives values of  $m = 5.3$  and  $c = -4.5$ , identical to the simple "add trendline" approach. An annotated spreadsheet containing all the equations in Excel format and full student-facing instructions are included in the Supplementary Information.

**Table 1. Data values for least-squares fitting**

Day	Number of flowers	Day	Number of flowers
1.0	2	0.0	1.5
2.0	5	0.5	1
3.0	10	1.5	3
4.0	18	2.5	8
		3.5	13
		4.5	21
		5.0	25

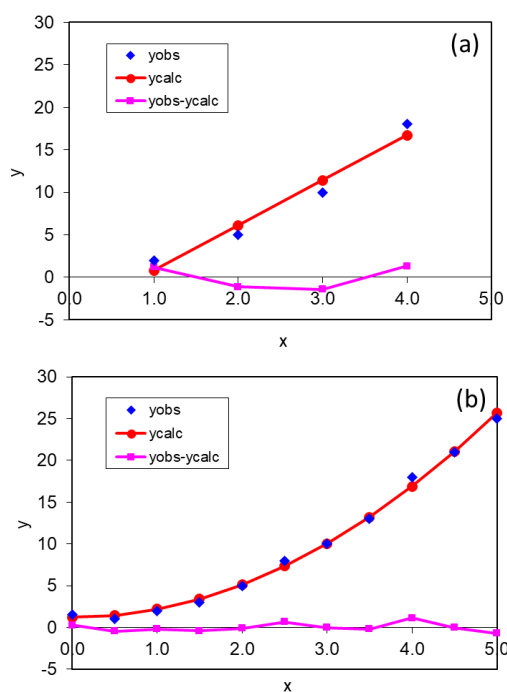


Figure 3. Fitting simple (a) linear and (b) polynomial functions in Excel.

With this linear example, it's also straightforward (but a little tedious) for students to do the least-squares analysis by-hand using simple matrix mathematics. This also lets them calculate the standard uncertainties on the refined parameters and the correlations between them. We find that students enjoy doing this exercise once in their lives, but rapidly realize why computers are generally used! This exercise is outlined in the Supplementary Information. The answers can be checked in Excel using its built-in linear least-squares array function "LINEST"; details on how to do this are again provided in the spreadsheet *solver\_linear\_fit*.

Figure 3b is a plot containing all of the data values contained in Table 1 and shows that the analysis just performed (using only a subset of the data) was rather naïve. If we look at the full data

---

set, where there are more observations collected over a larger  $x$  range, we see that a simple straight line fit is not appropriate. However, students can easily modify the Excel spreadsheet and try fitting the data to an expression such as  $y = mx^2 + c$ . This gives a much better fit. Note that at the end of this good least-squares fit the difference curve (pink) is scattered randomly around zero.

We find it useful to discuss the learning outcomes of this section with students. Some of these are:

1. Excel can be used to fit arbitrary non-linear functions to experimental data.
2. When performing data analysis, derived results are only reliable with an appropriate model.
3. Collecting data over as wide a set of conditions (here  $x$  values) as possible is important for testing the reliability of a given model. Later, students can explore the somewhat analogous problem of, for example, trying to simultaneously refine atomic displacement parameters and site occupancies in a Rietveld refinement over a limited  $2\theta$  range.
4. In a real analysis one would ideally have experimental uncertainties associated with each observation such that the statistical reliability of different models can be assessed.

## 5. FITTING GAUSSIAN AND LORENTZIAN PEAK SHAPES

Many analytical techniques give rise to signals recorded as peaks which can be described using either Gaussian or Lorentzian functions (Equations 11 and 12, respectively). Early low-resolution neutron powder diffractometers gave essentially Gaussian peaks. Most X-ray powder diffractometers give peak shapes that can be described by a mixture of Gaussian and Lorentzian functions, with the Lorentzian contribution often dominating.

The Excel sheet *solver\_fit\_gaussian* contains a simulated “experimental” data set which consists of a Gaussian function of intensity 500 units, *fwhm* 0.3 centered at  $x = 3.0$  with a small non-zero background and artificial experimental noise. Based on their learning from Section 4, students can use Equation 11, the variable parameters ( $pos \equiv 2\theta_{hkl}$ ,  $int$ ,  $fwhm$ ) to fit the peak, and a  $2\theta$ -dependent polynomial to fit the background. Instructions are given in the Excel sheet *solver\_fit\_gaussian*, and in a TA/Instructor-focused format in the Supplementary Information. An ideal fit is shown in Figure 4a.

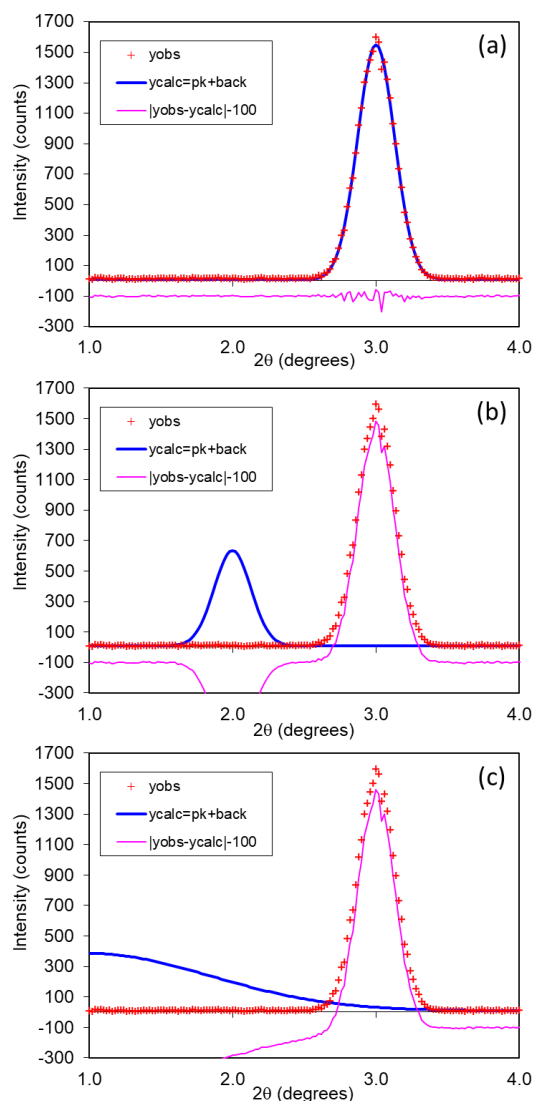


Figure 4. Fitting a Gaussian function in Excel. (a) shows the converged fit. (b) shows (*pos*, *int*, *fwhm* = 2.0, 200, 0.3), which does not converge. (c) shows (*pos*, *int*, *fwhm* = 1.0, 800, 2.0), which does converge.

Once they have a starting model, students should try starting values (*pos*, *int*, *fwhm* = 2.5, 200, 0.3) and use the Solver function to minimize  $\sum_i (y_{obs,i} - y_{calc,i})^2$  to fit the observed data. They should find the sum reduces rapidly from  $\sim 3 \times 10^7$  ( $R_{wp} \approx 106\%$ ) to  $2.8 \times 10^4$  ( $R_{wp} = 3.2\%$ ) in around 10 cycles. The minimization process can be followed in the bottom left of the Excel window. If they enable “Show Iteration Results” in the Solver options, they can follow each least-squares cycle graphically. The final fit should give (*pos*, *int*, *fwhm* = 3.0, 497, 0.3), and the difference curve should be randomly scattered around zero (Figure 4a). Note that students might get slightly different  $R_{wp}$  values with different models, if their refinements aren't fully converged or, potentially, with different Excel versions.

We use this example to let students test some of the convergence properties of least-squares fitting—that is how close the starting model needs to be for it to converge to the lowest  $R_{wp}$  minimum. This teaches how a “good model” can sometimes fail to converge to fit the data, whereas a “bad model” will converge. For example, Figures 4b and 4c show starting models with (b) ( $pos, int, fwhm = 2.0, 200, 0.3$ ),  $R_{wp} = 107\%$  and (c) ( $pos, int, fwhm = 1.0, 800, 2.0$ ),  $R_{wp} = 114\%$ . Students should find that despite the starting model in (c) being—visually and based on  $R_{wp}$ —a “worse starting model” than in (b), it will reliably converge. We ask students to test different starting models to come up with a criterion for reliable convergence. The simple observation in this case is that there needs to be some overlap between the *obs* and *calc* peaks. In other words, models like Figure 4b will generally diverge, but those like Figure 4c will converge as the blue line crosses the experimentally observed peak. Even a “terrible” starting model such as ( $pos, int, fwhm = 0.5, 2000, 10.0$ ) will usually converge if it meets this criterion, whereas seemingly more reasonable models will not. This helps students appreciate why it’s important to think about the best starting parameters to use in least-squares analysis; small manual adjustments are often needed before “blind” refinement. Later on (Section 6), they realize these ideas are crucial in performing a successful Rietveld refinement.

Students could be asked to set up a similar sheet to fit a Lorentzian function (Equation 12). A model answer is given in sheet *fit\_lorentzian\_answer*. They should see that the best-fit Lorentzian is, as expected, significantly worse than the best-fit Gaussian. Students should also see that an  $int = 500$  Lorentzian is narrower at its half height than a Gaussian, but has wider “tails”.

Peaks in a laboratory powder X-ray pattern are usually described well with a mixture of Gaussian and Lorentzian functions. One approach is to use the pseudo-Voigt formulation given in Equation 13 that contains a mixing parameter  $\eta$  ( $0 \leq \eta \leq 1$ ). Students can explore this in spreadsheet *fit\_pv\_answer* which uses a single peak from the X-ray diffraction pattern of  $TiO_2$  discussed below, and lets the student try fitting a Gaussian ( $G$ ), a Lorentzian ( $L$ ) or a  $\eta G + (1 - \eta)L$  pseudo-Voigt. This particular example fits well with  $\eta \approx 0.5$ . As Lorentzian broadening often dominates in many powder diffractometers, we use Lorentzian functions exclusively in later analysis.

---

## 6. WHOLE-POWDER-PATTERN FITTING: PEAKS, PAWLEY/LE BAIL AND RIETVELD REFINEMENT

With the basic ideas of peak fitting understood, students can explore whole-powder-pattern fitting methods. They do this initially using a simulated powder diffraction pattern of  $\text{TiO}_2$  so there are no issues caused by any systematic errors in a real data set. The simulation means that atomic displacement parameters can be ignored ( $B = 0$  in Equation 9), that they can use a constant background of  $\sim 26$  counts in the analysis and  $1/y_{\text{obs},i}$  weighting. We use a Lorentzian peak shape for simplicity.

Sheet *TiO2\_pkfit* and the accompanying student questions explore how the powder pattern from  $10\text{--}42^\circ$  can be fitted by summing four individual peaks of the type used in Section 5 and a simple background function (here a constant). By refining 13 parameters [a single background coefficient, and  $3 \times (\text{pos}, \text{int}, \text{fwhm})$  for the four reflections] students can get a good fit to the data with  $R_{\text{wp}} = 17.2\%$ . This is a good approach for extracting precise peak positions and intensities when peaks don't overlap. In this and later spreadsheets, the fit to the experimental data is presented graphically using a conventional "Rietveld plot" style. Observed data are shown as red points, the calculated pattern as a solid blue line, and the difference as an offset pink line. The  $2\theta_{hkl}$  values of each reflection are marked with a small triangle. It's worth noting that our fitting approach is computationally somewhat wasteful in that each peak is summed over the entire  $2\theta$  range. In most specialized Rietveld refinement software the  $2\theta$  range over which a peak contributes is limited to a narrower region close to  $2\theta_{hkl}$  for speed. Rietveld-specific software would, of course, also perform many of the calculations using loops, which leads to a much more compact description than our Excel approach.

Sheet *TiO2\_pawley* moves students one step closer to a Rietveld refinement. Here the peak intensities and widths are allowed to refine freely, but the peak positions are calculated from the unit-cell parameters via Equations 1 and 2 and a parameter to describe any peak offset. This is defined as a zero-point calibration ( $2\theta_{\text{true}} = 2\theta_{\text{obs}} - \text{zero}$ ), but in real experiments could be correcting for a minor error in mounted sample height. We draw the  $hkl$  tick marks at the  $2\theta_{\text{true}}$  position. Students can now refine the unit-cell parameters directly from the experimental data. The intensities (with Equation 5 corrections) could be used for either quantitative analysis in a multiphase sample, or to attempt structure solution. Note that we obtain  $R_{\text{wp}} = 17.2\%$  in this example, identical to that for the free peak



fitting approach, despite using one fitting parameter fewer. We typically set students a challenge problem of modifying the spreadsheet so that peak *fwhms* show a smooth  $2\theta$  dependence, further reducing the number of fitting parameters.

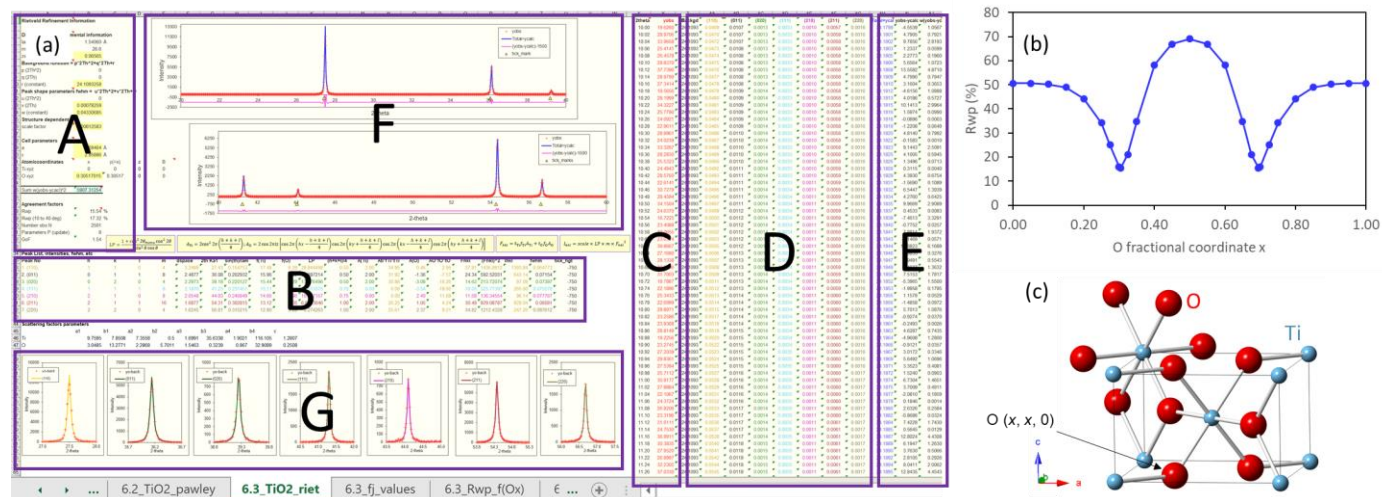


Figure 5. (a) Excel spreadsheet used for Rietveld refinement, with annotated sections discussed in the text. (b) Dependence of  $R_{wp}$  on fractional atomic coordinate  $x$  of O on site  $(x, x, 0)$ . (c) The rutile structure (Ti blue, oxygen red); oxygen sites in neighboring unit cells are included to show the coordination sphere around a Ti on one cell corner.

Sheet *TiO2\_riet* takes students all the way to a full Rietveld structural analysis. We will discuss it in some detail with reference to the annotated sheet in Figure 5a. Section **A** contains the parameters which are needed in the model. The diffractometer-related information includes the wavelength and monochromator angle (needed for the LP correction, Equation 10). Parameters  $p$ ,  $q$ , and  $r$  are used to describe a  $2\theta$ -dependent background polynomial (we continue using just term  $r$ ). Parameters  $u$ ,  $v$ ,  $w$  are used to describe a simple empirical  $2\theta$ -dependent peak *fwhm*. An overall scale factor is specified. Finally, the structural information is given in terms of unit-cell parameters  $a$  and  $c$  and the fractional atomic coordinates and displacement parameters ( $B$ ) of each atom in the asymmetric unit.

Section **B** contains the calculations that determine the position and intensity of each reflection. These replace the freely-refined values in earlier spreadsheets. Peak positions in degrees  $2\theta$  are calculated from the  $h$ ,  $k$ , and  $l$  Miller indices, cell parameters and wavelength using Bragg's law. The atomic scattering factors  $f_{Ti}$  and  $f_O$  are then calculated at this  $\sin\theta/\lambda$  value based on the parameters reported in International Tables Volume C<sup>43</sup> and ignoring anomalous scattering<sup>24</sup> (these are also plotted for the student in sheet *fj\_values*). The LP correction and structure factor  $F_{hkl}$  are then

---

calculated for each reflection. Equation 5 is used to calculate  $I_{hkl}$ , and the  $fwhm$  is calculated from  $u$ ,  $v$ ,  $w$  and  $2\theta_{hkl}$ .

365 As with the least-squares exercise by hand in Section 4, we find that it's instructive for students to calculate the  $I_{hkl}$  peak intensity for at least one reflection in this simple example "by-hand". This helps them engage and understand the equations and correction factors that feed into every-day crystallographic calculations. It, again, also teaches them why pre-written crystallography software is so convenient! This exercise is set in the Supplementary Information.

370 Section **C** contains the experimental data as columns of  $2\theta$  and  $y_{obs}$  and section **D** calculates the powder pattern. This is equivalent to the earlier examples, and contains a Lorentzian peak for each  $hkl$  reflection with the position (plus any  $2\theta_{zero}$  correction), intensity and  $fwhm$  calculated in Section **B**. Each  $hkl$  row/column combination of sections **B/D** is color-matched for clarity. The overall  $y_{obs}$  is then calculated in section **E** by summing each peak and the background function, and  $(y_{obs} - y_{calc})$  and  $w(y_{obs} - y_{calc})^2$  values calculated.

The bottom of section **A** contains the sum of the  $w(y_{obs} - y_{calc})^2$  column and should be minimized to perform a Rietveld refinement. This cell is shaded blue, and the parameters that might be refined are shaded yellow. The final sections **F** and **G** show the conventional Rietveld plots of observed, calculated and difference patterns for the whole dataset, and zooms of the seven individual  $hkl$  reflections.

380 We typically present the spreadsheet to students in the "fully refined" state, with  $R_{wp} = 15.5\%$ , though instructors might want to present a more approximate starting model so that students have to make refinement choices. These two possibilities are stored in Excel's "Data/What-If Analysis/Scenario Manager" as two different scenarios. We have included a suggested set of questions that students could explore in the Supplementary Information. These are deliberately set as challenge problems for students and explore topics such as:

- How does each individual parameters change the calculated pattern? How sensitive is the refinement to different parameters? How much can parameters be changed before the refinement no longer converges to the global minimum? When will a Rietveld refinement get "stuck" in a false minimum? Is there more than one model that can fit the experimental data?
- 390 Students are encouraged to generate plots such as Figure 5b, which shows the dependence of  $R_{wp}$  on the oxygen fractional atomic coordinate.

- 
- How sensitive are the important structural parameters to inadequacies in other aspects of the model? Which parameters are highly (or infinitely) correlated in a crystallographic refinement and potentially unreliable?
  - How can the spreadsheet be adapted to fit either neutron powder diffraction data or single crystal diffraction data? What are the pros and cons of these different experiments?
  - What structural information can be deduced from the Rietveld fit? What are the bond lengths and bond angles in the refined structural model? What is the connectivity pattern of the  $\text{TiO}_6$  octahedra? How does the structure help explain the high electronic conductivity of analogs like  $\text{VO}_2$ , and how might diffraction data be used to reveal structural changes when  $\text{VO}_2$  undergoes a metal to insulator transition on cooling?
  - Finally, we stated early in the paper that whilst the Rietveld method is generally used for structure refinement rather than structure solution, it is possible to solve structures *ab-initio* from powder data. Students are encouraged to explore how Excel can be used to start refinements from different random starting models and essentially solve the crystal structure from scratch. Whilst this is a trivial example, remarkably complex unknown structures have been solved with this type of approach.<sup>25, 44-46</sup>

Students should also be asked to consider the reliability of the Rietveld structural fit. The most important indicator of the correctness of a Rietveld fit is the visual inspection of the match between the calculated and observed patterns.<sup>25</sup> All observed reflections should be explained by the model and their relative intensities correctly described. No unfitted extra reflections should be observed. As students explore in S.I. Problem 6.6, minor features in the difference curve due to the approximate peak shape model can usually be ignored, provided the over- and under-calculated areas are comparable. It is difficult to make quantitative conclusions on the uncertainty in the refined O x coordinate as the peak shape issues lead to correlated ( $y_{\text{obs}} - y_{\text{calc}}$ ) residuals. As such, the Rietveld-derived standard uncertainty (here  $\sim 0.0005$ ) is almost certainly an underestimate of the true uncertainty.<sup>25</sup> However, the shape of an  $R_{\text{wp}}$  plot like that of Figure 5b, and the sensible geometry of the Rietveld-derived structure gives confidence in the model's reliability.

Students should also consider the fact that this exercise was limited to the first seven peaks in the powder diffraction to keep the spreadsheet manageable. In a normal Rietveld analysis one would analyze data to a higher  $2\theta$ , thus including many more  $hkl$  reflections. This would improve the reliability of the derived parameters and help reduce correlations between parameters which give

different  $I_{hkl}$  dependencies on  $2\theta$  (e.g. site occupancies give no direct  $2\theta$  dependence, temperature factors do via Equation 9). This is somewhat analogous to Figures 3a and 3b, where the wider  $x$  range in Figure 3b clearly showed a non-linear model is required.

Students going on to perform Rietveld refinement as part of their research might want to analyze the same data set in one of the mainstream Rietveld software packages. The supplementary information contains the files needed to perform equivalent Rietveld analysis in TOPAS or GSAS-1.<sup>34</sup>

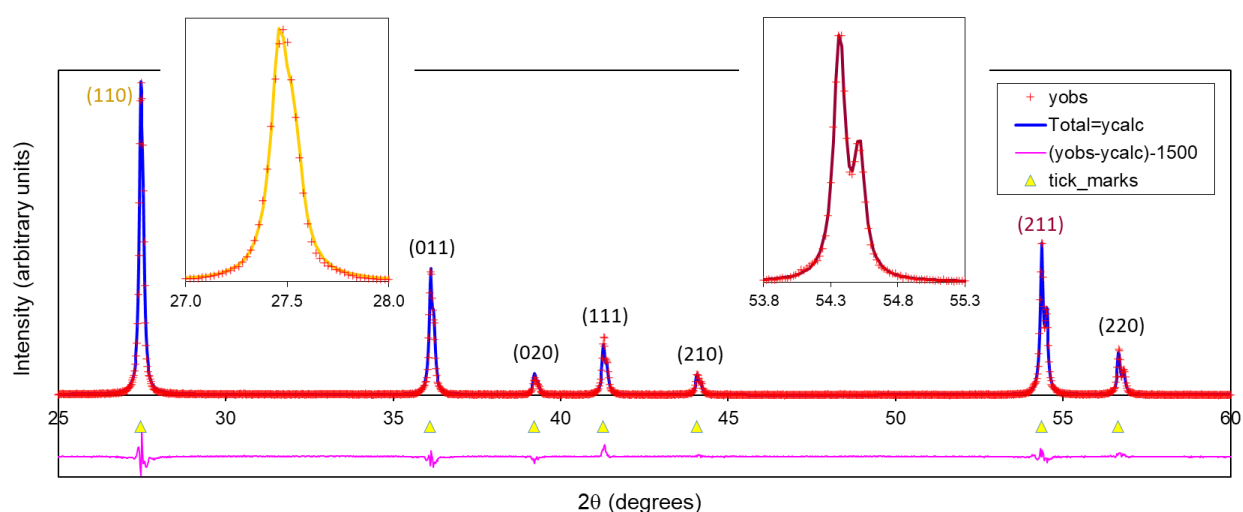


Figure 6. Rietveld fit to experimental data discussed in Section 7. Observed data shown as red crosses, calculated as a solid blue line and the difference curve (offset) as a pink line. Arrows show the predicted  $2\theta$  values of different  $hkl$  reflections. Insets show zooms of the (110) and (211) reflections. Note how the  $K_{\alpha 1/\alpha 2}$  radiation leads to clear peak splitting at higher  $2\theta$ .

## 7. RIETVELD REFINEMENT WITH REAL EXPERIMENTAL DATA

Sheet *TiO2\_riet\_real\_data* takes the analysis one step further and engages students with real experimental data. Students can use this sheet to analyze data collected on a typical laboratory instrument. The example dataset provided was collected in ~30 minutes on a Siemens d5000 diffractometer with a pyrolytic graphite diffracted beam monochromator and point detector (i.e. a very much non-state-of-the-art instrument). The experimental set up introduces one additional complication in that the X-ray tube produces a mixture of  $\text{Cu } K_{\alpha 1}$  and  $K_{\alpha 2}$  radiation with wavelengths of 1.5406/1.5445 Å that reach the detector in a ~2:1 ratio.<sup>51</sup> This means that a pair of closely-spaced peaks are observed for each  $hkl$  reflection in the powder diffraction pattern. This is treated in the sheet *TiO2\_riet\_real\_data* by summing a second Lorentzian peak, with intensity scaled by the value of

---

$K_{\text{ratio}} = 0.5$ , at position  $2\theta_{hkl}$  for  $K_{\alpha 2}$  radiation. Scattering factors and intensity corrections are assumed  
445 to be unchanged relative to  $K_{\alpha 1}$  radiation.

Students can perform similar analysis to that described in Section 6 on either the experimental data set provided, or an equivalent data set of their own collected as part of a laboratory practical. Pop-up comments on the various spreadsheet cells suggest sensible instrumental parameter values for other common experimental set ups. A typical final Rietveld plot is shown in Figure 6. Student  
450 exercises which explore the experimentally-derived structure and discuss its relevance to understanding physical properties are given in the Supplementary Information.

## 8. CLASSROOM EXPERIENCE AND ANALYSIS OF EFFECTIVENESS

The Excel Rietveld spreadsheet was originally developed for a biennial international graduate student training school that the authors have co-run with colleagues from the ESRF and UCL since  
455 2004. Students on the five-day residential school come from a wide range of disciplines (chemistry, archaeology, earth sciences, engineering, materials, pharmacy, physics, industry, etc) with very different backgrounds and prior training. In the earliest schools we taught using a traditional combination of formal lectures and detailed “how to do this refinement” exercises in common Rietveld packages. Our experience was that even by the end of the school many students had little  
460 understanding of the physical meaning of different “tick box” parameters used in data fitting. This reflects a lack of deep or critical learning, and leaves students unable to tackle new or more challenging problems. We now adopt a teaching model which involves relatively concise content delivery through lectures or reading (~25% of time), time (~25%) for students to undertake by-hand problem solving exercises working in small groups, and ~50% of time working in a computer lab—a  
465 time-on-task focus. The material described in this article is one of the early computer exercises, and has been completed by over 400 students. Given the very different background of students we let them work through the exercises independently at their own speed. We staff the computer lab with ~1 TA per 12 students, and TA time ends up roughly evenly split between giving specific how-to guidance to the less experienced students and setting/discussing challenge problems with those more  
470 experienced. In this environment we make no attempt to assess students in a traditional “did they get the right answer and complete all the problems” sense. We also encourage them to set their own

---

goals. For some students performing an independent fit to a single Gaussian peak (Section 5) is as valuable as exploring all the aspects of Rietveld analysis in a real experimental data set (Section 7) is to others.

475 Our emphasis when discussing the exercise with the class is the bottom-up approach of building up ideas and complexity (Figure 1). For example: Section 4 starts students with the basics of linear least-squares fitting and sets a challenge of fitting arbitrary non-linear functions; Section 5 introduces a peak shape function and sets a student-challenge to also add in a function to describe experimental background; Section 6 (sheets 6.1 and 6.2) generalizes to multiple peaks, with a student challenge to  
480 describe smoothly-varying peak shapes; sheet 6.3 finally combines all the ideas into a full Rietveld fit. Students also identify issues associated with inappropriate models or fitting approaches in early simple examples, which they can reapply in the more complex Rietveld examples. We find that the common question of “Why didn’t this refinement work?” when students later attempt much more complex refinements can usually be answered with a response such as: “Think back to exercise 5.2,  
485 why didn’t that work?”. Whilst it would be possible to work through these ideas in other software packages or in specialist Rietveld software, we chose Excel as the one package that almost all students are familiar with, and that they can almost certainly access. We have lost count of the number of times students have said “I didn’t know Excel could do this”, or the number who have said they can now see how to apply similar approaches to analyze other data.

490 Our assessment of the effectiveness of the approach is judged via pre- and post-course questionnaires to assess the background and confidence levels of students before the school against their experiences of the different teaching activities. The residential nature of the school also means we can discuss learning informally during meal breaks and non-academic sessions. Student feedback is uniformly that the experience of working through a complex data analysis problem from scratch  
495 helps cement fundamental ideas and identifies knowledge-gaps that they might otherwise skip over. Students comment explicitly that the Excel-based exercises lead to better understanding of what Rietveld software packages do, and nurture a more critical approach to their use.

Whilst we have used these exercises primarily with undergraduate and postgraduate research students, they could readily form part of a senior level practical experiment or inquiry-based mini

---

project. This would give students the experience of working all the way from an analytical measurement through to a quantitative three dimensional structural model. This will, *inter alia*, help them appreciate the origin of much of the information they learn about interatomic bond distances and coordination geometry, which is so fundamental to chemistry and other disciplines. Even for students not likely to perform powder diffraction or crystallographic analysis later in their careers, the data analysis philosophy taught is widely re-applicable. The Excel exercises described here are also mirrored in separate online tutorials using Rietveld-specific refinement software.<sup>52</sup> These allow students continuing to work with powder diffraction data to build from this specific simple example to much more challenging problems. Our website provides over 100 such problems for students to explore.<sup>52</sup>

## 9. CONCLUSIONS

In conclusion, we believe that the self-guided exploratory study program set out in this paper allows a student with no prior knowledge of data analysis, no computer-coding expertise and only a basic background in crystallography to reach the point where they can perform a full structural analysis on a compound from scratch. For most students this will be the first time they fully understand how the beautiful structural models drawn in their text books are derived. Whilst the process is necessarily reasonably involved, we find that it is well within the capability of undergraduate students. The bottom-up approach adopted allows students to test ideas on simple examples, which are later reapplied as the complexity of the problem necessarily increases. We believe that this experiential learning leads to much better student understanding than other approaches.<sup>53</sup> The ideas we explore are widely re-applicable in other areas of data analysis.

## ASSOCIATED CONTENT

### Supporting Information

Supporting Information is available on the ACS Publications website at DOI:

10.1021/acs.jchemed.XXXXXXX [ACS will fill this in] and contains: An Excel spreadsheet containing all the examples discussed in the paper (XLSX). Student exercises to do linear regression by hand and to calculate the intensity of the (020) reflection of TiO<sub>2</sub>; Instructor notes on the spreadsheet contents; Instructor notes containing specific student exercises for a computer lab, challenge-problems and

---

discussion points. Detailed instructions and annotated spreadsheet on linear function fitting for students with no previous experience in using Excel's Solver function; Simulated neutron powder diffraction pattern of TiO<sub>2</sub> (DOCX). TOPAS and GSAS format files allowing analysis of the same data set used here in Rietveld-specific software (.ZIP containing various text files for software packages).

#### Corresponding Author

\*E-mail: john.evans@durham.ac.uk

#### ACKNOWLEDGMENTS

We thank the generations of students who have attended the Durham Powder Diffraction and Rietveld Refinement school for extensive testing (and occasional breaking) of the Excel spreadsheet presented; and Andy Fitch (European Synchrotron Radiation Facility, ESRF), Jeremy Cockcroft (University College London, UCL) and many school tutors for feedback on their experiences using it as a teaching tool. We thank the Powder Diffraction Commission of the IUCr, Durham University and Bruker for on-going support of the school and EPSRC and Panalytical for supporting early schools. We thank the BBC for broadcasting the show "Strictly Come Dancing" during which the Excel Rietveld spreadsheet was started.

#### REFERENCES

1. Taylor, R.; Wood, P. A., A Million Crystal Structures: The Whole Is Greater than the Sum of Its Parts. *Chem. Rev.* **2019**, *119*, 9427–9477.
2. Inorganic Crystal Structure Database – ICSD. <https://icsd.products.fiz-karlsruhe.de/> (accessed November 2020).
3. International Centre for Diffraction Data PDF. <https://www.icdd.com/> (accessed November 2020).
4. Sojka, Z.; Che, M., Presentation and Impact of Experimental Techniques in Chemistry. *J. Chem. Educ.* **2008**, *85* (7), 934–940.
5. Hoggard, P. E., Integrating Single Crystal X-Ray Diffraction in the Undergraduate Curriculum. *J. Chem. Educ.* **2002**, *79* (4), 420–421.
6. Hulien, M. L.; Lekse, J. W.; Rosmus, K. A.; Devlin, K. P.; Glenn, J. R.; Wisneski, S. D.; Wildfong, P.; Lake, C. H.; MacNeil, J. H.; Aitken, J. A., An Inquiry-Based Project Focused on the X-ray Powder Diffraction Analysis of Common Household Solids. *J. Chem. Educ.* **2015**, *92* (12), 2152–2156.
7. Battle, G. M.; Ferrence, G. M.; Allen, F. H., Applications of the Cambridge Structural Database in Chemical Education. *J. Appl. Crystallogr.* **2010**, *43* (5 Part 2), 1208–1223.



- 
- 560 8. Grazulis, S.; Sarjeant, A. A.; Moeck, P.; Stone-Sundberg, J.; Snyder, T. J.; Kaminsky, W.; Oliver, A. G.; Stern, C. L.; Dawe, L. N.; Rychkov, D. A.; Losev, E. A.; Boldyreva, E. V.; Tanski, J. M.; Bernstein, J.; Rabeh, W. M.; Kantardjieff, K. A., Crystallographic Education in the 21st Century. *J. Appl. Crystallogr.* **2015**, *48* (6), 1964–1975.
9. Pett, V., Teaching Crystallography to Undergraduate Physical Chemistry Students. *J. Appl. Crystallogr.* **2010**, *43*, 1139–1143.
- 565 10. Kantardjieff, K. A.; Kaysser-Pyzalla, A. R.; Spadon, P., Crystallography Education and Training for the 21st Century. *J. Appl. Crystallogr.* **2010**, *43*, 1137–1138.
11. Toby, B. H., Observations on Online Educational Materials for Powder Diffraction Crystallography Software. *J. Appl. Crystallogr.* **2010**, *43*, 1271–1275.
- 570 12. Brannon, J. P.; Ramirez, I.; Williams, D.; Barding, G. A.; Liu, Y.; McCulloch, K. M.; Chandrasekaran, P.; Stieber, S. C. E., Teaching Crystallography by Determining Small Molecule Structures and 3-D Printing: An Inorganic Chemistry Laboratory Module. *J. Chem. Educ.* **2020**, *97* (8), 2273–2279.
13. Zheng, S.-L.; Campbell, M. G., Connecting Key Concepts with Student Experience: Introducing Small-Molecule Crystallography to Chemistry Undergraduates Using a Flexible Laboratory Module. *J. Chem. Educ.* **2018**, *95* (12), 2279–2283.
- 575 14. Campbell, M. G.; Powers, T. M.; Zheng, S.-L., Teaching with the Case Study Method To Promote Active Learning in a Small Molecule Crystallography Course for Chemistry Students. *J. Chem. Educ.* **2016**, *93* (2), 270–274.
- 580 15. Wilson, C. C.; Parkin, A.; Thomas, L. H., Frontiers of Crystallography: A Project-Based Research-Led Learning Exercise. *J. Chem. Educ.* **2012**, *89* (1), 34–37.
16. Rosenthal, J., Spreadsheet Calculations for X-ray powder Diffraction Patterns. *J. Chem. Educ.* **1991**, *68* (11), A285–A286.
17. Stojilovic, N.; Isaacs, D. E., Inquiry-Based Experiment with Powder XRD and FeS<sub>2</sub> Crystal: “Discovering” the (400) Peak. *J. Chem. Educ.* **2019**, *96* (7), 1449–1452.
- 585 18. Corsepius, N. C.; DeVore, T. C.; Reisner, B. A.; Warnaar, D. L., Using Variable Temperature Powder X-ray Diffraction To Determine the Thermal Expansion Coefficient of Solid MgO. *J. Chem. Educ.* **2007**, *84* (5), 818–821.
19. Longo, E.; Espinosa, J. W. M.; Souza, A. G.; Lima, R. C.; Paris, E. C.; Leite, E. R., Structural Order–Disorder Transformations Monitored by X-ray Diffraction and Photoluminescence. *J. Chem. Educ.* **2007**, *84* (5), 814–817.
- 590 20. Varberg, T. D.; Skakuj, K., X-ray Diffraction of Intermetallic Compounds: A Physical Chemistry Laboratory Experiment. *J. Chem. Educ.* **2015**, *92* (6), 1095–1097.
21. Ismail, M. N., Hydrothermal Synthesis and Characterization of Titanosilicate ETS-10: Preparation for Research Integrated Inorganic Chemistry Laboratory Course. *J. Chem. Educ.* **2020**, *97* (6), 1588–1594.
- 595

22. Pires, J., Simple Analysis of Historical Lime Mortars. *J. Chem. Educ.* **2015**, 92 (3), 521–523.
23. Martín-Ramos, P.; Susano, M.; Gil, F. P. S. C.; Pereira da Silva, P. S.; Martín-Gil, J.; Silva, M. R., Facile Synthesis of Three Kobolds: Introducing Students to the Structure of Pigments and Their Characterization. *J. Chem. Educ.* **2018**, 95 (8), 1340–1344.
24. Dinnebier, R. E.; Leineweber, A.; Evans, J. S. O., *Rietveld Refinement, Practical Powder Diffraction Pattern Analysis using TOPAS*. De Gruyter: 2018; p 331.
25. McCusker, L.; Von Dreele, R.; Cox, D.; Louër, D.; Scardi, P., Rietveld Refinement Guidelines. *J. Appl. Crystallogr.* **1999**, 32 (1), 36–50.
26. Young, R. A., *The Rietveld Method*. Oxford University Press: 1993.
27. Matching online tutorials.  
[http://community.dur.ac.uk/john.evans/topas\\_workshop/tutorial\\_riet\\_excel.htm](http://community.dur.ac.uk/john.evans/topas_workshop/tutorial_riet_excel.htm) (accessed November 2020).
28. Blake, A. J.; Cole, J. M.; Evans, J. S.; Main, P.; Parsons, S.; Watkin, D. J., *Crystal Structure Analysis: Principles and Practice*. Oxford University Press: 2009.
29. Clegg, W., *Crystal Structure Determination*. Oxford University Press: 1998.
30. Giacovazzo, C.; Monaco, H. L.; Viterbo, D.; Scordari, F.; Gilli, G.; Zanotti, G.; Catti, M., *Fundamentals of Crystallography*. Oxford University Press: 2002.
31. *International Tables for X-Ray Crystallography, Volume I Symmetry Groups* Kynoch Press: 1969.
32. Evans, J. S. O.; Evans, I. R., Beyond Classical Applications of Powder Diffraction. *Chem. Soc. Rev.* **2004**, 33 (8), 539–547.
33. Pecharsky, V.; Zavalij, P., *Fundamentals of Powder Diffraction and Structural Characterization of Materials*. Springer Science & Business Media: 2008.
34. Dinnebier, R. E.; Billinge, S. J., *Powder Diffraction: Theory and Practice*. Royal Society of Chemistry: 2008; p 574.
35. Rietveld, H. M., Line Profiles of Neutron Powder-Diffraction Peaks for Structure Refinement. *Acta Crystallogr.* **1967**, 22 (1), 151–152.
36. Rietveld, H. M., A Profile Refinement Method for Nuclear and Magnetic Structures. *J. Appl. Crystallogr.* **1969**, 2 (2), 65–71.
37. Rietveld, H. M., The Rietveld method. *Phys. Scr.* **2014**, 89 (9), 098002.
38. van Laar, B.; Schenk, H., The Development of Powder Profile Refinement at the Reactor Centre Netherlands at Petten. *Acta Crystallogr., Sect. A* **2018**, 74 (2), 88–92.
39. Le Bail, A., Whole Powder Pattern Decomposition Methods and Applications: A Retrospection. *Powder Diffr.* **2005**, 20 (4), 316–326.
40. Le Bail, A.; Duroy, H.; Fourquet, J., *Ab-initio* Structure Determination of LiSbWO<sub>6</sub> by X-ray Powder Diffraction. *Mater. Res. Bull.* **1988**, 23 (3), 447–452.
41. Pawley, G., Unit-cell Refinement from Powder Diffraction Scans. *J. Appl. Crystallogr.* **1981**, 14 (6), 357–361.

42. David, W. I.; Shankland, K.; Baerlocher, C.; McCusker, L., *Structure Determination from Powder Diffraction Data*. Oxford University Press: 2002.
43. Wilson, A. J. C., *International Tables for Crystallography. Volume C: Mathematical, Physical and Chemical Tables*. Kluwer Academic Publishers (published for the International Union of Crystallography): Dordrecht/Boston/London, 1992; p 883.
44. David, W. I. F.; Shankland, K., Structure determination from Powder Diffraction Data. *Acta Crystallogr., Sect. A* **2008**, 64 (1), 52–64.
45. Favre-Nicolin, V.; Cerny, R., FOX, 'Free Objects for Crystallography': a Modular Approach to *Ab Initio* Structure Determination from Powder Diffraction. *J. Appl. Crystallogr.* **2002**, 35 (6), 734–743.
46. Harris, K. D., Powder Diffraction Crystallography of Molecular Solids. In *Advanced X-Ray Crystallography*, Springer: 2011; pp 133–177.
47. Coelho, A. A., TOPAS and TOPAS-Academic: an Optimization Program Integrating Computer Algebra and Crystallographic Objects Written in C++. *J. Appl. Crystallogr.* **2018**, 51 (1), 210–218.
48. Coelho, A. A.; Evans, J. S. O.; Evans, I. R.; Kern, A.; Parsons, S., The TOPAS Symbolic Computation System. *Powder Diffr.* **2011**, 26 (4), S22.
49. Larson, A. C.; Von Dreele, R. B. GSAS; Los Alamos National Laboratory, New Mexico, 1994.
50. Toby, B. H., EXPGUI, a Graphical User Interface for GSAS. *J. Appl. Crystallogr.* **2001**, 34 (2), 210–213.
51. Stojilovic, N., Using Cu K $\alpha_1$ /K $\alpha_2$  Splitting and a Powder XRD System To Discuss X-ray Generation. *J. Chem. Educ.* **2018**, 95 (4), 598–600.
52. Online powder diffraction analysis tutorials.  
[http://community.dur.ac.uk/john.evans/topas\\_workshop/tutorial\\_menu.htm](http://community.dur.ac.uk/john.evans/topas_workshop/tutorial_menu.htm) (accessed November 2020).
53. Svinicki, M. D.; McKeachie, W. J., Experiential Learning: Case-Based, Problem-Based and Reality-Based. In *McKeachie's Teaching Tips: Strategies, Research and Theory for College and University Teachers*, 14 ed.; Svinicki, M. D.; McKeachie, W. J., Eds. Wadsworth: Belmont, CA, 2015.